JMB
Journal of Microbiology and Biotechnology

Online ISSN : 1738-8872
Pirnt ISSN : 1017-7825

JMB Papers in Press. First Published online Oct 10, 2018
DOI: 10.4014/jmb.1712.12026

Manuscript Number: JMB17-12026

Title: Zinc Ions Affect Siderophore Production by Fungi Isolated from the Panax schinseng Rhizosphere

Article Type: Research article

Keywords: Root-associated fungi, siderophores, Zn2+, penicillium commune

Zinc Ions Affect Siderophore Production by Fungi Isolated from the *Panax ginseng* Rhizosphere

Khalid Abdallah Hussein[1,2], Jin Ho Joo[2,*]

[1]Botany and Microbiology Department, Faculty of Science, Assiut University, 71516, Assiut, Egypt

[2]Department of Biological Environment, Kangwon National University, Chuncheon, Kangwon-do, Republic of Korea

*Corresponding author:

Jin Ho Joo PhD,

Mailing address: Department of Biological Environment, Kangwon National University, 192-1, Hyoja 2-dong, Chuncheon, Kangwon-do, 200-701, Republic of Korea

Phone: +82-33-250-6448

Fax: +82-33-241-6640

Email address: jhjoo@kangwon.ac.kr

Abstract

Although siderophore compounds are mainly biosynthesized as a response to iron deficiency in the environment, they also bind with other metals. A few studies demonstrated prompting impact of heavy metals on the siderophore-mediated iron uptake by microbiome. Here, we investigated siderophore production by a variety of rhizosphere fungi under different concentrations of Zn^{2+} ion. These strains were specifically isolated from the rhizosphere of *Panax ginseng* (Korean ginseng). The siderophore production of isolated fungi was investigated with chrome azurol S (CAS) assay liquid media amended with different concentrations of Zn^{2+} (50 to 250 µg mL^{-1}). The percentage of siderophore units was quantified using the ultra-violet (UV) irradiation method. The results indicated that high concentrations of Zn^{2+} ion increase the production of siderophore in iron-limited cultures. Maximum siderophore production by the fungal strains was detected at Zn^{2+} ion concentration of 150 µg mL^{-1} except for *Mortierella* sp., which had the highest siderophore production at 200 µg mL^{-1}. One potent siderophore-producing strain (*Penicillium* sp. JJHO) was strongly influenced by the presence of Zn^{2+} ions and showed high identity to *P. commune* (100% using 18S-rRNA sequencing). The purified siderophore of the *Penicillium* sp. JJHO strain was chemically identified using UV, Fourier-transform infrared spectroscopy (FTIR), and matrix-assisted laser desorption/ionization time-of-flight mass spectrometer (MALDI-TOF-MS) spectra.

Keywords: Root-associated fungi, Siderophore, Zn^{2+}, *Penicillium commune*

Introduction

Iron is one of the most frequent components of the Earths' crust. It is available in the soil, with rare exceptions, as oxide hydrates, which have little dissociation constants [1]. In recent years, the production of siderophore by fluorescent pseudomonads in the rhizosphere has received great attention, due to their prospective role in the promotion of plant growth and bio-control of soil-borne diseases [2]. Most fungi produce siderophore [1], with few exceptions (e.g., *Saccharomyces* species); nevertheless, *Saccharomyces cerevisiae* uses exotic siderophore [3]. Fungi produce a variety of siderophore, mainly hydroxamate. Biosynthesis expression and the uptake systems of siderophore are regulated by internal iron concentrations. However, siderophore forms a complex with metals other than iron, such as actinides [4]. Dimkpa et al. [5] found that Al, Cd, Ni, and Cu stimulate the production of three different hydroxamate siderophore; namely, desferrioxamine B, desferrioxamine E, and coelichelin by *Streptomyces* sp. Tripathi et al. [6] stated that the inoculation of *Phaseolus vulgaris* with a Cd- and Pb-resistant and siderophore producer strain of *Pseudomonas putida* KNPP enhanced plant growth, with cadmium and lead having no side effects on plant quality compared to the control. Various studies have assessed the concentration of Fe^{2+} and other heavy metal ions on siderophore-mediated iron uptake by microorganisms [5]. However, only a few studies have assessed the effect of Zn^{2+} ion concentrations on iron uptake. High concentrations of Zn^{2+} are toxic, inhibiting the aerobic respiratory chain [7]. Metal-resistant siderophore-producing microorganisms play a distinctive role in the survival and promotion of plant growth in contaminated soils, by decreasing metal toxicity and providing plants with iron and other nutrients. Because of rapid industrial development, there is growing public concern over the potential accumulation of heavy metals in soils. The Zn content of farmland soils is frequently higher than that of natural soils. This phenomenon is mainly due to the application of commercial fertilizers,

65 manure, and/or liming materials [8]. In addition, pesticides and fungicides containing Zn
66 contribute to its presence in agricultural soils. Zn in agricultural soils sometimes accumulates to
67 reach values considerably higher than its optimum concentration as a nutrient, and it may be toxic
68 to soil organisms [9]. The primary function of siderophore is to chelate Fe(III). They also form
69 complex compounds with other heavy metals, such as Cd(II), Cu(II), and Zn(II) [10]. The ability
70 to form complexes depends on the functionality of ligands, with several studies focusing on how
71 siderophore impacts the mobility of these metals in the environment [11, 12]. Thus, siderophore
72 represents a valuable and environmentally friendly tool for removing metals from the soil. The
73 present study investigated how Zn^{2+} influences siderophore production by a variety of rhizosphere
74 fungal strains. In addition, the siderophore of a strong siderophore-producing strain was purified,
75 identified, and characterized before possible siderophorogenic application to promote plant growth.
76
77
78 **Materials and methods**
79 **Micro-organisms and culture conditions**

80 Soil samples were collected from the rhizosphere of ginseng, *Panax ginseng*, which is an
81 important economic herb cultivated and used in Asia. The medicinal and commercial value of
82 ginseng was discovered over ten centuries ago. Samples were collected in zipper bags and stored
83 at 4 °C. Twenty-three fungal strains belonging to different classes were isolated using the dilution
84 plate technique and purified on Czapek's Agar medium containing 3% saccharose, 0.2% sodium
85 nitrate, 0/1% dipotassium phosphate, 0.05% magnesium sulfate, 0.05% potassium chloride, 0.001%
86 ferrous sulfate, and 1.5% agar. Stock cultures of fungi were preserved on 2% malt extract agar
87 (MEA) slants grown at 27 °C, and stored at 4 °C before screening for siderophore.

Qualitative Chrome Azurol S (CAS) assay for siderophore production

The fungal strains were sub-cultured on MEA slant tubes and incubated at 27 °C. Five days later, the culture spores were scraped aseptically into sterile distilled water containing 0.1% Tween 80 and were homogenized with a vortex. A cell counting Neubauer chamber (Merck, Madrid, Spain) was used. The spore concentration was adjusted to 1.0×10^6 conidia/mL. 10 mL of iron-free Czapek Dox Broth (pH 7.3), and was inoculated with 1 mL of the spore suspension. The cultures were incubated in shakers at 150 rpm and 27 °C for 7 days. CAS-agar (100 mL) was prepared according to Schwyn and Neilands [13]. A 7.5 mL volume of 2 mM Chrome Azurol S was mixed with 1.5 mL iron solution (1 mM $FeCl_3.6H_2O$, 10 mM HCl). While stirring, 6.0 mL of 10 mM hexadecyl trimethyl ammonium bromide (HDTAB) solution was added, and the resulting blue solution was kept at 50 °C. In addition, buffer solution was prepared using 0.6 gm of PIPES (piperazine-N,N′-bis [2-ethanesulfonic acid]) dissolved in 85 mL deionized water, and was adjusted to a final pH of 6.7 using 6M KOH. To this solution, 1.5 g agar was added and dissolved by heating it at 50 °C. The blue and agar solutions were finally mixed. The Petri dishes (9 cm diameter) were prepared with 20 mL CAS-agar. After gelling, 5 mm diameter holes were made and dried for 2 h at 31 °C. Each hole was filled with 100 µl culture supernatant. A non-inoculated media was used as the negative control, and the cell-free supernatants from fungal cultures were tested [14]. Plates were left overnight at 4 °C, of which only the seven most clear positive strains were used in the subsequent analyses (Fig. 1).

Effect of zinc ions on siderophore production

The fungal isolates were tested against different concentrations of Zn^{2+} ions, ranging between 50 and 250 µg mL^{-1} using $ZnSO_4$ in Czapek Dox Broth media (pH 7.3). Rhizobacteria strain

Pseudomonas aeruginosa was selected from our previous study [15], and was stressed under the same concentrations of Zn^{2+} ions in Tris minimal media (pH 6.8). The pH was adjusted to 6.8 with 0.1 M Pipes. The cultures were agitated to a stationary phase in the deferrated media. A 0.5 mL CAS test solution was added to 0.5 mL culture supernatant and 10 µl shuttle solution (0.2 M 5-sulfosalicylic acid) and was mixed thoroughly. The mixture was left for 5 min. The color development was assessed by absorbance (A_{630}) for the loss of blue color. A sterile culture medium was used as a blank, while the non-inoculated medium, CAS, and shuttle solutions were used as references. The siderophore units were evaluated by the following principle:

$$[(Ar-As)/Ar] \times 100 = \% \text{ siderophore units}$$

where (Ar) is the absorbance value of the reference, and (As) is the absorbance value of the sample. The investigation was conducted in three replicates. The average of the three replicates was used for all analyses.

Identification of strains

The fungi strains were identified provisionally by direct microscopic examination and culture characteristics according to Qi [16], Kong [17], and Zhang [18]. To a 1.5 mL Eppendorf tube containing 500 mL lysis buffer (400 mM Tris-HCl [pH 8.0], 60 mM ethylene diaminetetra acetic acid [EDTA] [pH 8.0], 150 mM NaCl, 1% sodium dodecyl sulfate), and a small lump of mycelia from young cultures were added with a sterile toothpick. The toothpick was also used to disrupt the lump of mycelia. The tube was left at room temperature for 10 min. After adding 150 mL potassium acetate (pH 4.8; which was made from 60 mL of 5 M potassium acetate, 11.5 mL glacial acetic acid, and 28.5 mL distilled water), the tube was briefly vortexed and spun at 10000 rpm for 1 min. The supernatant was transferred to another 1.5 mL Eppendorf tube and centrifuged again.

After transferring the supernatant to a new 1.5 mL Eppendorf tube, an equal volume of isopropyl alcohol was added. The tube was mixed by gentle inversion, spun at 10000 rpm for 2 min, and the supernatant was discarded. The resulting pellet of DNA was washed in 300 mL of 70% ethanol. Then, the pellet was spun at 10000 rpm for 1 min, and the supernatant was discarded. The air-dried DNA pellet was dissolved in 50 mL of deionized H_2O, and 1 mL of the purified DNA was used in 25 to 50 mL of PCR mixture. The extractions were completed in duplicate for each sample. The universal primers used for fungal amplification were ITS1: 5′ TCC GTA GGT GAA CCT GCG G 3′ and ITS4: 5′-TCCTCCGCTTATTGATATGC-3′ [19]. PCR amplification was performed in a thermal cycler for 30 cycles using denaturation of DNA at 94 ºC for 1 min, primer annealing at 56 ºC for 30 sec, and primer extension at 72 ºC for 1 min. The PCR product was sequenced at Macrogene Company. To identify the isolated fungi, the partial gene sequence was matched with the full sequence presented in the GenBank database via the BLAST search (NCBI). The fungal 18S rRNA gene fragments were aligned using Clustral W [20]. Sequence alignment and phylogenetic analysis with homologous genes were performed using DNAstar software (version 5.01).

Extraction and purification

The culture was centrifuged and the pH of the supernatant was decreased to pH 2.0 by 12 M HCl and was then extracted with 0.4 volume of ethyl acetate. The fractions of ethyl acetate were collected and concentrated by a rotary vacuum evaporation. The concentrated dried fractions were dissolved in deionized H_2O before column purification. Fifty grams of Sephadex LH-20 was suspended in methanol with shaking for about 30 min. The suspension was poured into a glass column of 50 x 1.5 cm diameter and was equilibrated by four-bed volumes of methanol. The sample was concentrated and loaded onto the column and eluted by methanol that was four-bed

volumes of the column. Separated fractions were placed in 100 mL flasks to test the extracted siderophore using aluminum backed TLC plates coated with a 0.25 mm layer of silica gel using solvent system acetic acid:water:butanol (3:5:12, v/v). Iron-binding compounds were identified by spraying the TLC plates with CAS assay reagent. Autoclave-sterilized filter paper discs (10 mm diameter) was also impregnated with Sephadex LH-20 purified siderophore solution (15 µl). The discs were placed using sterile forceps on CAS-Agar plate. Color development around the discs was determined after incubation overnight at 4 °C. Positive fractions were collected together and dried by the rotary vacuum evaporator, and were then lyophilized and stored at -20 °C. The Csáky and Arnow [21, 22] assays were also performed to differentiate between catechol and hydroxamate type siderophore.

Spectra analysis instruments

Matrix-Assisted Laser Desorption/Ionization Time-of-Flight Mass Spectrometer (MALDI-TOF-MS) analysis was performed by adopting positive ion mode on a time-of-flight mass spectrometer (Bremen, Daltonics Bruker, Microflex), with a 1.25-m flight tube. Desorption/ionization was acquired by using a 337-nm nitrogen laser with a 3-ns pulse width. Available acceleration potential was +20kV on average. The spectra included in this paper represent a range of 100–200 laser shots. Laser power was fixed to be slightly beyond the threshold, to obtain a good determination and signal-to-noise ratios. The analysis was repeated at least three times to check reproducibility. The absorption spectra of the constituents were detected using a UV–vis spectrometer (Perkin Elmer) from 300–700 nm. Transmission infrared spectra were obtained via KBr plates (4000–400 cm^{-1}) on 8300 FT-IR spectrophotometers.

Statistical analysis

All results were statistically analyzed using the SAS package (ver. 9.1). Means of three replicates were subjected to one-way ANOVA [23].

Results

Siderophore-producing strains

A total of 23 isolates were selected at random based on differences in the morphological features of the colonies for further study. The strongest siderophore-producing strain, *Penicillium* sp. JJHO was subjected to siderophore purification. *Penicillium* sp. JJHO had a high identity (99% using 18S-rRNA sequencing) to *P. commune*. It was characterized by slow growth on MEA, with a grey-green colony and blue conidia. The 18S rRNA analysis showed that the isolate of *Penicillium* sp. JJHO had 100% nucleotide base homology with *P. commune*. The structure of the phylogenetic tree was produced by the online tool PhyML (www.phylogeny.fr), and visualization of the tree was achieved using TreeDyn. The ribosomal RNA sequence of *Penicillium* sp. JJHO was saved in the NCBI GeneBank under the accession number KC549672. Details of the phylogenetic affiliation of the representative sequence for *Penicillium* sp. JJHO strain are shown in (Fig. 2).

Effect of Zn ions on siderophore production

The effect of Zn^{2+} on the siderophore of the studied microbial strains was quantified using a universal CAS assay [14]. Supernatants containing the siderophore of each sample were identified by a typical pinkish-red color. Zn^{2+} ions influenced the production of the siderophore of all of the

studied microbial strains. The optimum siderophore production by the fungal strains was detected at a Zn^{2+} ion concentration of 150 µg mL^{-1}, except for *Mortierella* sp., which had the highest siderophore production of 39.62% of units at 200 µg mL^{-1}. *Penicillium* sp. JJHO and *Metarhizium anisopliae* had the highest siderophore production, producing 72.65 and 72.43% of units, respectively. *Rhodosporidium toruloides* and *Trichoderma* sp. were the most strongly influenced by the presence of the Zn^{2+} ions in the defferated media. The former produced 13.76 and 18.52% of the units in the control and at 50 µg mL^{-1} Zn^{2+} ion, respectively, while *Trichoderma* sp. produced 33.11 and 63.73 % of the units, in the control and at 50 µg mL^{-1} Zn^{2+} ion, respectively. *Fusarium oxysporum* had almost the same siderophore production at 150 and 200 µM mL^{-1} concentration of Zn^{2+} ions, producing 68.76 and 68.62% of units, respectively. At a 250 µg mL^{-1} concentration of Zn^{2+} ions, the two fungal strains (*Rhodosporidium toruloides* and *Mortierella turficola*) had the lowest siderophore production compared to the control. Otherwise, the siderophore production of most of the fungal isolates was significantly higher than that of the control (Table 1). *Trichoderma* sp. produced 18.52% of the siderophore units in the control and 63.39% of siderophore units in the 250 µg mL^{-1} Zn^{2+} treatment. However, the bacterial specimen *Pseudomonas aeruginosa* produced 36.9 % of the units in the control and 25.05% of the units in the 250 µg mL^{-1} Zn^{2+} treatment (lower than the control). The bacterium *P. aeruginosa* only had the highest siderophore production at 100 µg $mL^{-1}Zn^{2+}$ concentration, whereas the fungal strain *Trichoderma* sp. had the highest production at 150 µg mL^{-1} Zn ion concentration.

Extraction and spectra analysis of *Penicillium* sp. JJHO siderophore

The siderophore of *Penicillium* sp. JJHO strain was only positive to the Csalky test. However, *Pseudomonas aeruginosa*, a rhizobacterial example, showed a positive reaction to Arnow's assay. These results confirm the presence of hydroxamate siderophore and catecholate types in these two

strains, respectively. The highest siderophore production of fungi was shown by *Penicillium* sp. JJHO which produced 72.65 % of units. Ten fractions were obtained through a chromatography separation column by Sephadex LH-20. An impregnated filter paper disc from each fraction was placed on the CAS Agar plate. Only the fractions that turned the blue CAS Agar to a clear orange or yellow color were used. Using acetic acid:water:butanol (3:5:12, v/v) as the mobile phase, iron-binding compounds were confirmed by spraying the TLC plates with CAS assay solution. UV spectra of the Sephadex LH-20 purified fungal siderophore showed that absorption peaked at 425 nm (Fig. 3A, B). Ferrichrome at the excitation wavelength (425 nm) showed blue fluorescence (Fig. 3C). FT-IR spectra (Fourier Transform Infrared Spectroscopy) of the compound indicated the presence of an amide (NH-C=O), which is the main functional group in the compound. The compound was investigated from the peaks at wavelengths of 1640, 1680, 3500 cm^{-1} and was assigned as N-H bending, C=O stretching, and N-H stretching, respectively (Table 2). The chelation or coordination of the compound with Fe (III) occurred via the acidic bond of the nitroso group N-O, which was investigated at 1490 cm^{-1} and 1150 cm^{-1}, and was assigned as an asymmetric stretch (strong) and a symmetric stretch (strong), respectively (Fig. 3D). Ferrichrome has a molecular formula of $C_{27}H_{42}N_9O_{12}$, producing a molecular weight of 740.52 g/mol. Based on the detected MALDI spectra, the molecular weight peaked at 763.0 Da as $[Ferrichrome+Na]^+$ (Fig. 4).

Discussion

Microorganisms with the most effective siderophore-mediated iron uptake have a competitive advantage and are of use for biocontrol and as biofertilizers. Heavy metals have an extreme effect on siderophore production. The presence of Co, Cd, and Zn in the media improved the production of siderophore, whereas Mn and Mo decreased production [5]. Specific nutrients are required for

siderophore secretion, and might vary from one microorganism to another; however, iron-controlled conditions stay unchanged, contributing an energetic role in its secretion [24].

This study demonstrated the impact of Zn^{2+} ion concentrations on siderophore production by a variety of fungi. Optimum siderophore production by the fungal strains was attained at Zn^{2+} ion concentrations of 150 µg mL^{-1}, except for *Mortierella* sp., which had the highest siderophore production of 39.62 % units at 200 µg mL^{-1}. Our previous studies showed that *P. aeruginosa* is one of the most important PGPR strains, producing 76.53% of siderophore units [15]. *Trichoderma harizianum* is a key PGPF and biocontrol agent, exhibiting high siderophore production [25]. In the current study, *Trichoderma* sp. TR274, as well as a bacterial specimen, showed the strong effect of Zn ions on the induction of siderophore. Thus, in contrast to bacterial strain, fungal strains showed higher siderophore production at a 250 µg mL^{-1} concentration of Zn^{2+}. (Fig. 5). There are two possible explanations for the motivating impact of heavy metals on siderophore biosynthesis. First, heavy metals might be required in the siderophore biosynthesis pathway or their control [26]. Second, the amount of free siderophore might decline when complexes are formed with heavy metals ions. Thus, soluble iron concentration is also diminished. As iron does not stimulate the generation of siderophore, more siderophore molecules would then be delivered [5].

The biochemical pathway of ferrichrome synthesis is poorly understood. At concentrations of 250 µg mL^{-1} Zn^{2+} ions, only two fungal isolates showed lower and significant siderophore production than the control. *Trichoderma* sp. produced 18.52% of siderophore units in the control and 63.39% of siderophore units in the 250 µg mL^{-1} Zn^{2+} treatment. Moreover, *P. aeruginosa* produced 36.95% of units in the control and 25.05% of units in the 250 µg mL^{-1} Zn^{2+} treatment.

Zn^{2+} is of great importance for microorganisms and is a catalytic co-factor for many proteins, including Zn^{2+} finger DNA-binding proteins. Zn^{2+} is also an intracellular additional messenger in many signal transduction pathways [27]. Furthermore, superoxide dismutases (SODs) in fungi are essential for the detoxification of reactive oxygen species (ROS) generated by host cells, and are zinc-dependent enzymes [28]. Consequently, in iron, there is competition for Zn^{2+} ions [29]. Fungi secrete a variety of hydroxamate siderophore. The synthesis of ferrichrome has been characterized for one member of the Ascomycete and Basidiomycete classes [30]. This class of siderophore includes other compounds, such as ferrichrome, ferricrocin, ferrichrome A, ferrichrome B, and malonichrome [31].

Most ferrichrome siderophore compounds are cyclic hexapeptides that play vital functions in fungal biochemistry [31]. Ferricrocin promotes the germination of asexual spores of *Neurospora crassa* by storing iron reserves inside the spores [32]. This activity is similar to the role of ferrichrome-type in the asexual reproduction of *A. nidulans* [33] and *P. chrysogenum* [32]. The fungal siderophore structures are mostly hydroxamates, which are similar to bacterial siderophore [34]. Fungal hydroxamates have similar biosynthetic pathways because of their similar basic unit, Nd-acyl-Nd-hydroxy ornithine [35]. Frisvad and Larsen [36] found that *A. fumigatus* produces a peptide synthetase that is essential for the ferrichrome production. Miethke and Marahiel [37] detected L-cis-ferrichrome in *P. parvum,* while [35] detected it in *N. crassa*, *A. quadricinctus*; however, the authors were not able to recognize D-cis-ferrichrome.

The siderophore produced by organisms might be restricted to a particular structural family; however, in a few cases, the fungus biosynthesizes siderophore that belongs to different structural families [4]. Taxonomic studies of Ustilaginales showed that *Tilletiaria*, *Graphiola*, *Protomyces*, and parasitic Ustilaginales form ferrichrome-type siderophore, whereas saprophytic Ustilaginales

form rhodotorulic acid [27, 38]. The investigation of the fungal siderophore of *Penicillium* sp. JJHO using UV and Fluorescence Spectroscopy data in this study showed an absorption peak at a wavelength of 425 nm. Also, the compound at the excitation 425 nm wavelength showed blue fluorescence. These results suggest the presence of Ferrichrome. Masuda et al. [39] suggested that ferrichrome shows peak absorption at 425 nm. Ferrichrome was stirred at 25 °C in a 1 mL cell, and the excitation wavelength (λ_{exc}) was set at 425 nm, with fluorescence emission (λ_{em}) being measured at 500 nm, confirming the results obtained by Hannauer et al. [40].

The FTIR of the compound extracted from *Penicillium* sp. JJHO showed that the compound displayed three peaks at wave numbers 1640,1680, and 3500 cm^{-1}, which were assigned as N-H stretching, C=O stretching, and, N-H bending, respectively. The chelation or coordination of the compound with Fe (III) occurs via the acidic bond of the nitroso group N-O. This group was investigated at 1490 cm^{-1} and 1150 cm^{-1}, which were assigned as an asymmetric stretch (strong) and symmetric stretch (strong), respectively. Ferrichrome is a cyclic hexapeptide made out of three glycines and three adjusted ornithine residues that unite Fe(III) with the hydroxamate groups [-N(OH)C(=O)C-].

Ferrichrome was initially isolated in 1952, and was observed to be delivered by the fungi genera *Aspergillus*, *Ustilago*, and *Penicillium* [41]. The main functional group in the compound is the amide (NH-C=O). The cellular siderophore of *A. nidulans* are ferricrocin and triacetylfusigen. However, *P. chrysogenum* contains ferrichrome. The conidia of both species (*A. nidulans* and *P. chrysogenum*) lack siderophore at high salt concentrations [42]. Kröber et al. [43] showed that *Trichophyton rubrum* produces the same siderophore ferrichrome C and ferricrocin, as well as *Microsporum gypseum*, *M. audouinii*, and *M. canis*. In comparison, *T. tonsurans* and *T. mentagrophytes* only produce ferrichrome [42].

316 Filamentous ascomycete genomes mostly contain one or two nonribosomal peptide
317 synthetases (NRPS). However, *Botrytis cinerea* might possess three ferrichrome synthetases of
318 NRPS [44]. Bushley and Turgeon, 2010 characterized the subfamilies of fungal NRPSs. Their
319 analyses suggested that mono/bimodular NRPSs have more early origins and more conserved
320 domain architectures than most multi-modular NRPSs. Phylogenetic analyses of ferrichrome
321 synthetases provided support for an ancestral duplication event, producing two main families. The
322 authors also supported the hypothesis that siderophore synthetases are derived from a hexamodular
323 ancestral gene, likely created by the tandem doubling of complete NRPS modules [45].

324 Correlations between the types and taxonomy of siderophore have been demonstrated in
325 bacteria. However, there is a weak correlation between siderophore generation and taxonomic
326 classification in fungi [4]. Our study showed that, based on the MALDI-TOF spectra of the fungal
327 siderophore, the characteristics of ferrichrome (M.Wt 763.0 Da) can be assigned as
328 $[Ferrichrome+Na]^+$. Ferrichrome has the molecular formula of $C_{27}H_{42}N_9O_{12}$, which gives a
329 molecular weight of 740.52 g/mol.

330 Siderophore binds to other metals, in addition to binding strongly with Fe(III). Because of
331 their metal-chelating ability, there might be potential applications for siderophore in medical and
332 environment-associated problems [4]. Siderophore types are also being investigated for other
333 applications, including the decorporation of actinides, as anticancer and antimicrobial agents, and
334 for transporting drugs into microorganisms [4]. In conclusion, it is necessary to understand the
335 chemistry and biology of siderophore before applying them or their analogs to the field of
336 agriculture. Heavy metals affect the siderophore production of microbes. By analyzing the effect
337 of Zn^{2+} on siderophore production in fungi, we showed that Zn^{2+} ions alone are able to activate
338 siderophore synthesis in microbes. According to UV spectra, FTIR, and MALDI-TOF data, the

investigated fungal siderophore produced by the *Penicillium* sp. JJHO strain is likely to be the hydroxamate-type ferrichrome. The presence of adequate quantities of heavy metals might promote plant growth.

Conflicts of interest

The authors declare no conflicts of interest.

Acknowledgment

This work was supported by the National Research Foundation of Korea (NRF) grant funded by the Korea government (Ministry of Science, ICT & Future Planning) (No.2017R1A2B1009738).

References

1. Pereg L, McMillan M. 2015. Scoping the potential uses of beneficial microorganisms for increasing productivity in cotton cropping systems *Soil. Biol. Biochem.* **80:** 349-358.
2. Neubauer U, Nowack B, Furrer G, Schulin R. 2000. Heavy metal sorption on clay minerals affected by the siderophore desferrioxamine B. *Environ. Sci. Technol.* **34:** 2749–2755.
3. Aznar A, Dellagi A. 2015. New insights into the role of siderophores as triggers of plant immunity: what can we learn from animals? *J. Exper. Bot.* **66:** 3001–3010,
4. Renshaw JC, Robson GD, Trinci APJ, Wiebe MG, Livens FR, Collison D, Taylor RJ. 2002. Fungal siderophores structures, functions and applications. *Mycol. Res.* **106:** 1123-1142.
5. Dimkpa CO, Svatos A, Dabrowska P, Schmidt A, Boland W, Kothe E. 2008. Involvement of siderophores in the reduction of metal-induced inhibition of auxin synthesis in *Streptomyces* spp. *Chemosphere.* **74:** 19–25.

6. Tripathi M, Munot HP, Shouche Y, Meyer JM, Goel R. 2005. Isolation and functional characterization of siderophore-producing lead- and cadmium-resistant *Pseudomonas putida* KNP9. *Curr. Microbiol.* **50:** 233–237.
7. Bazihizina TC, MartiL RA, Spinelli F, Giordano C, Caparrotta S, Gori M, Azzarello E, Mancuso S. 2014. Zn^{2+} induced changes at the root level account for the increased tolerance of acclimated tobacco plants. *J. Exp. Bot.* **65:** 4931-4942.
8. Kabir E, Ray S, Kim K, Yoon H, Jeon E, Kim Y, Cho Y, Yun S, Brown JC. 2012. Current Status of Trace Metal Pollution in Soils Affected by Industrial Activities. *Sci. World J.* Article ID 916705, 18 pages.
9. Liu M, Lia Y, Zhanga W, Yaojing W. 2013. Assessment and Spatial distribution of zinc pollution in agricultural soils of Chaoyang, China. *Procedia Environ. Sci.* **18:** 283-289.
10. Johnstone TC, Nolan EM. 2015. Beyond iron: non-classical biological functions of bacterial siderophores. *Dalton Trans.* **14:** 6320-6339.
11. Saha M, Sarkar S, Sarkar B, Sharma BK, Bhattacharjee S, Tribedi P. 2016. Microbial siderophores and their potential applications: a review. *Environ. Sci. Pollut. Res. Int.* **23:** 3984-3999.
12. Ahmed E, Holmstrom SJM. 2014. Siderophores in environmental research: roles and applications: minireview. *Microb. Biotechnol.* **7:** 196-208.
13. Schwyn B, Neilands, J.B. 1987. Universal chemical assay for the detection and determination of siderophores. *Analy. Biochem.***160:** 47-56.
14. Naidu AJ, Yadav M. 1997. Influence of iron, growth temperature and plasmids on siderophore production in *Aerornonas hydrophila*. *J. Med. Microbiol*. **47:** 833-838.

15. Hussein KA, Joo JH. 2017. Stimulation, purification, and chemical characterization of siderophores produced by the rhizospheric bacterial strain *Pseudomonas putida. Rhizosphere* **4:** 16-21

16. Qi Z. 1997. Fungi of China: *Aspergillus* and Related Teleomorphs vol. 5. Beijing: Science Publisher.

17. Kong H. 2007. Fungi of China (Vol. 35): *Penicillium* and Related Teleomorphs. Beijing: Science Publisher.

18. Zhang Z. 2003. Fungi of China (Vol. 14): Gladaxporism, Fusicladium, Pyricularia. Beijing: Science Publisher.

19. Herlemann DP, Labrenz M, Jürgens K, Bertilsson S, Waniek JJ, Andersson AF. 2011. Transitions in bacterial communities along the 2000 km salinity gradient of the Baltic Sea. *ISEM J.* **5:** 1571-1579.

20. Thompson J, Higgins D, Gibson T. 1994. Clustal W: improving the sensitivity of progressi ve multiple sequence alignment through sequence weighting, positionspecific gap penaltie s and weight matrix choice. *Nucleic Acids Res.* **22:** 4673-4680.

21. Csáky TZ. 1948. On the estimation of bound hydroxylamines in biological materials. *Acta. Chem. Scand.* **2:** 450-454.

22. Arnow LE. 1937. Colorimetric determination of the components of 3,4-dihydroxyphenylalanine tyrosine mixtures. *J. Biol. Chem.* **118:** 531-537.

23. SAS Institute Inc, SAS, SAS/STAT® 9.1 User's Guide. 2004. SAS Institute Inc., Cary, NC, USA.

24. Ahmed E, Holmström SJM. 2014. Siderophores in environmental research: roles and applications *Microb. Biotechnol.* **7:** 196-208.

405 25. Hussein KA, Joo JH. 2012. Comparison between Siderophores Production by Fungi Isolated
406 from Heavy Metals Polluted and Rhizosphere Soils. *Korean J. Soil Sci. Fert.* **45:** 798-804.
407 26. Rajkumar M, Freitas H. 2009. Effects of inoculation of plantgrowth promoting bacteria on
408 Ni uptake by Indian mustard. *Biores. Technol*. **99:** 3491-3498.
409 27. Yamasaki S, Sakata-Sogawa K, Hasegawa A. 2007. Zinc is a novel intracellular second
410 messenger. *J. Cell Biol.* **177:** 637-645.
411 28. Huang J, Canadien V, Lam GY. 2009. Activation of antibacterial autophagy by NADPH
412 oxidases. *Natl. Acad. Sci.* **106:** 6226-6231.
413 29. Corbin BD, Seeley EH, Raab A. Feldmann J, Miller MR, Torres VJ, Anderson KL, Dattilo
414 BM, Dunman PM, Gerads R, Caprioli RM, Nacken W, Chazin WJ, Skaar EP. 2008. Metal
415 chelation and inhibition of bacterial growth in tissue abscesses. *Science* **15:** 962-965.
416 30. Schwecke T, Goettling, K, Durek P, Duenas I, Kaeufer NF, Zock ES, Staub E, Neuhof T,
417 Dieckmann R, Doehren H. 2006. Nonribosomal peptide synthesis in *Schizosaccharomyces*
418 *pombe* and the architectures of ferrichrome-type siderophore synthetases in fungi. *Chem.*
419 *biochem.* **7:** 612-622.
420
421 31. Rossbach S, Wilson TL, Kukuk ML, Carty HA. 2000. Elevated zinc induces siderophore
422 biosynthesis genes and a zntA-like gene in *Pseudomonas fluorescens. FEMS Microbiol.*
423 *Lett.* **1:** 61-70.
424 32. Carroll CS, Nesbitt JR, Henry KA, Pinto LJ, Moinzadeh M, Scott JK, Moore MM. 2012.
425 Structural Requirements for the Activity of the MirB Ferrisiderophore Transporter of
426 *Aspergillus fumigates* Isabelle Raymond-Bouchard. *Eukaryot Cell*. **11:** 1333–1344.

33. Eisendle M, Oberegger H, Zadra I, Haas H. 2003. The siderophore system is essential for viability of Aspergillus nidulans: functionalanalysis of two genes encoding l-ornithine N 5-monooxygenase (sidA) and a non-ribosomal peptide synthetase (sidC). *Mol. Microbiol.* **49:** 359-375.

34. Plattner H, Diekmann H. 1994. Enzymology of siderophore biosynthesis. In Metal Ions in Fungi (G. Winkelmann & D. R. Winge, eds) 99-116. Marcel Dekker, New York.

35. Gründlinger M, Yasmin S, Lechner BE, Geley S, Schrett M, Hynes M, Haas H. 2013. Fungal siderophore biosynthesis is partially localized in peroxisomes. *Mol. Microbiol.* **88:** 862–875.

36. Frisvad JC, Larsen TO. 2016 Extrolites of *Aspergillus fumigatus* and Other Pathogenic Species in Aspergillus Section Fumigati. *Front. Microbiol.* **6:** 1485.

37. Miethke M, Marahiel MA. 2007. Siderophore-Based Iron Acquisition and Pathogen Control *Mol. Biol. Rev.* **71:** 3413-4511.

38. Weaver RS, Kirchman DL, David A. 2003. Hutchins Utilization of iron/organic ligand complexes by marine bacterioplankton Aquatic Microbial Ecology. *Aquat. Microb. Ecol.* **31:** 227-239,

39. Masuda T, Hayashi J, Tamagaki S. 2000. C_3-symmetric ferrichrome-mimicking Fe^{3+}complexes containing the 1-hydroxypyrimidinone Fe^{3+} binding moieties based on α-cyclodextrin: helicities in solvent environments. *J. Chem. Soci. Perkin Trans.* **2:** 161-167.

40. Hannauer M, Barda Y, Mislin GA, Shanzer A, Schalk IJ. 2010. The Ferrichrome Uptake Pathway in *Pseudomonas aeruginosa* Involves an Iron Release Mechanism with Acylation of the Siderophore and Recycling of the Modified Desferrichrome. *J. Bacteriol.* **192:** 1212-1220.

41. Tedstone AA, Lewis DJ, Brien P. 2016. Synthesis, Properties, and Applications of Transition Metal-Doped Layered Transition Metal Dichalcogenides. *Amer. Chem. Mat.* **28:** 1965-1974.

42. Dimkpa C. 2016. Microbial siderophores: Production, detection and application in agriculture and environment. *Endocytobiosis Cell Res.* **27:** 7-16.

43. Kröber A, Scherlach K, Hortschansky P, Shelest E, Staib P, Kniemeyer O, Brakhage Axel A. 2016. HapX Mediates Iron Homeostasis in the Pathogenic Dermatophyte *Arthroderma benhamiae* but Is Dispensable for Virulence. *PLoS ONE* **11:** e0150701.

44. Bushley KE, Ripolland DR, Turgeon B. 2008. Module evolution and substrate specificity of fungal nonribosomal peptide synthetases involved in siderophore biosynthesis. *BMC Evolutionary Biol.* **8:** 328.

45. Bushley KE, Turgeon BG, 2010. Phylogenomics reveals subfamilies of fungal nonribosomal peptide synthetases and their evolutionary relationships. *BMC Evol. Biol.* **10:** 26.

Table 1. Zn^{2+} effect on siderophore synthesis by several fungal species

Fungal Strain	Class	Zn^{2+} Concentration					
		0 μg mL^{-1}	50 μg mL^{-1}	100 μg mL^{-1}	150 μg mL^{-1}	200 μg mL^{-1}	250 μg mL^{-1}
Aspergillus versicolor Mir	Ascomycetes	55.35±0.20b	48.19±0.13d	58.76±0.20a	59.54±0.40a	53.06±0.26b	50.91±0.40c
Penicillium commune JJHO	Ascomycetes	67.37±0.26d	69.42±0.33c	69.46±0.26c	72.65±0.27a	70.95±0.27b	69.42±0.15c
Mortierella turficola CQ1	Zygomycetes	32.19±0.20d	33.55±0.26c	31.06±0.39e	37.96±0.33b	39.62±0.33a	34.46±0.23c
Fusarium oxysporum FCHA	Ascomycetes	46.65±2.16b	66.93±0.46a	67.36±0.26a	68.76±0.53a	68.62±0.77a	66.15±0.77a
Metarhizium anisopliae KHAU	Ascomycetes	68.63±0.46c	69.02±0.38c	71.25±0.20b	72.43±0.40a	71.86±0.50ab	58.71±0.52d
Rhodosporidium toruloides K-1-8	Basidiomycota	13.76±0.39e	33.11±0.15b	33.21±0.15b	34.82±0.27a	31.45±0.69c	22.49±0.46d
Trichoderma harzianum TR274	Ascomycetes	18.52±0.72d	63.73±0.30c	66.01±0.59b	67.63±0.60a	65.27±0.47b	63.39±0.33c

Means with the same letter within a row are not significantly different at $P<0.05$.

Table 2. FT-IR of the function groups in ferrichrome

Classes	Function groups	Bands
Amines	N-H stretch (1 per N-H bond)	3400
	N-H bend	1500
	C-N Stretch (alkyl)	1200
	N-H bend (oop)	~800
Amides	N-H stretch	3500
	C=O stretch	1680-1630
	N-H bend	1640-1550
Carboxylic acids	O-H stretch	3400
	C=O stretch	1700
	C-O stretch	1210

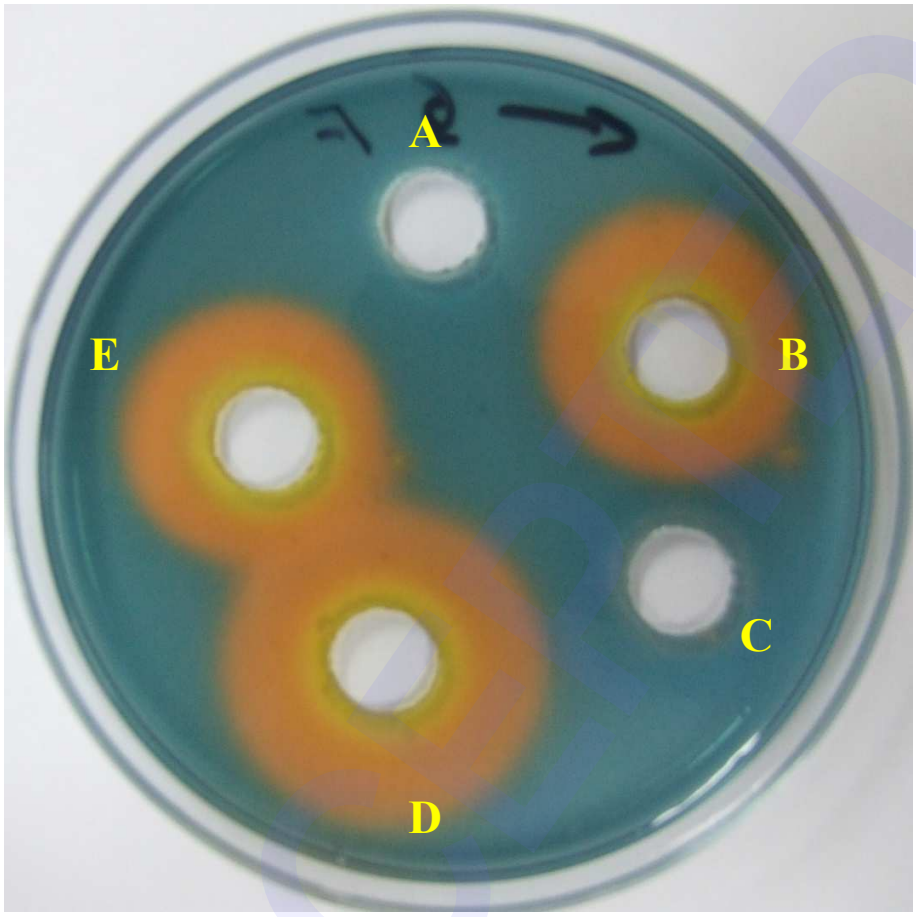

Fig. 1. CAS-agar diffusion (CASAD) assay to determine the most clear positive strains were used in the subsequent analyses. (A) Control (non-inoculated medium). (B) *Penicillium commune* JJHO. (C) *Saccharomyces cerevisiae* K2S2 (negative fungal strain). (D) *Metarhizium anisopliae* KHAU. (E) *Trichoderma harzianum* TR274.

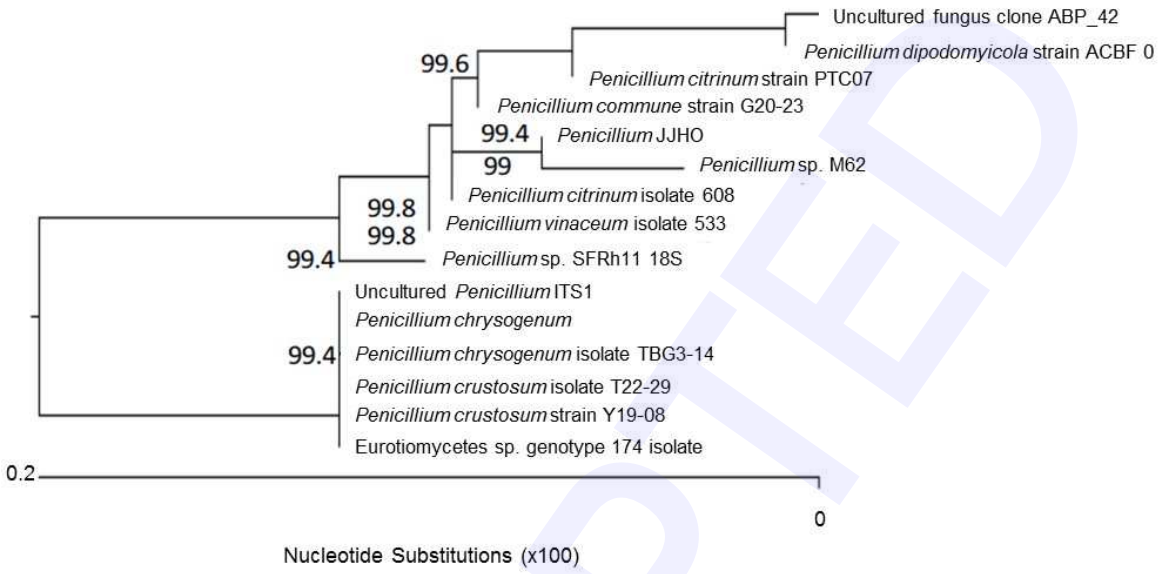

Fig. 2. Phylogenetic tree designed by neighbor-closing analysis of 18S rRNA gene sequence to show the position of *Penicillium* JJHO the siderophore producer isolate among the genus *Penicillium*. *P. commune* (GU723445), *P. chrysogenum* (JX139710), *P. crustosum* (HQ262518), *P. dipodomyicola* (GQ161752), *Eurotiomycetes* sp (JQ761933), *P. citrinum* (JN206678), *P. chrysogenum* (JF731274), *Penicillium* sp. (HQ443258), Uncultured *Penicillium* (FN394532), Uncultured fungus clone ABP_42 (JF497145), *Penicillium* sp. (HM573339), *P. crustosum* (GU134895), *P. vinaceum* (DQ681340), *P. citrinum* (DQ681331), *P. rubens* (JX003126), *Eupenicillium crustaceum* (AB479321).

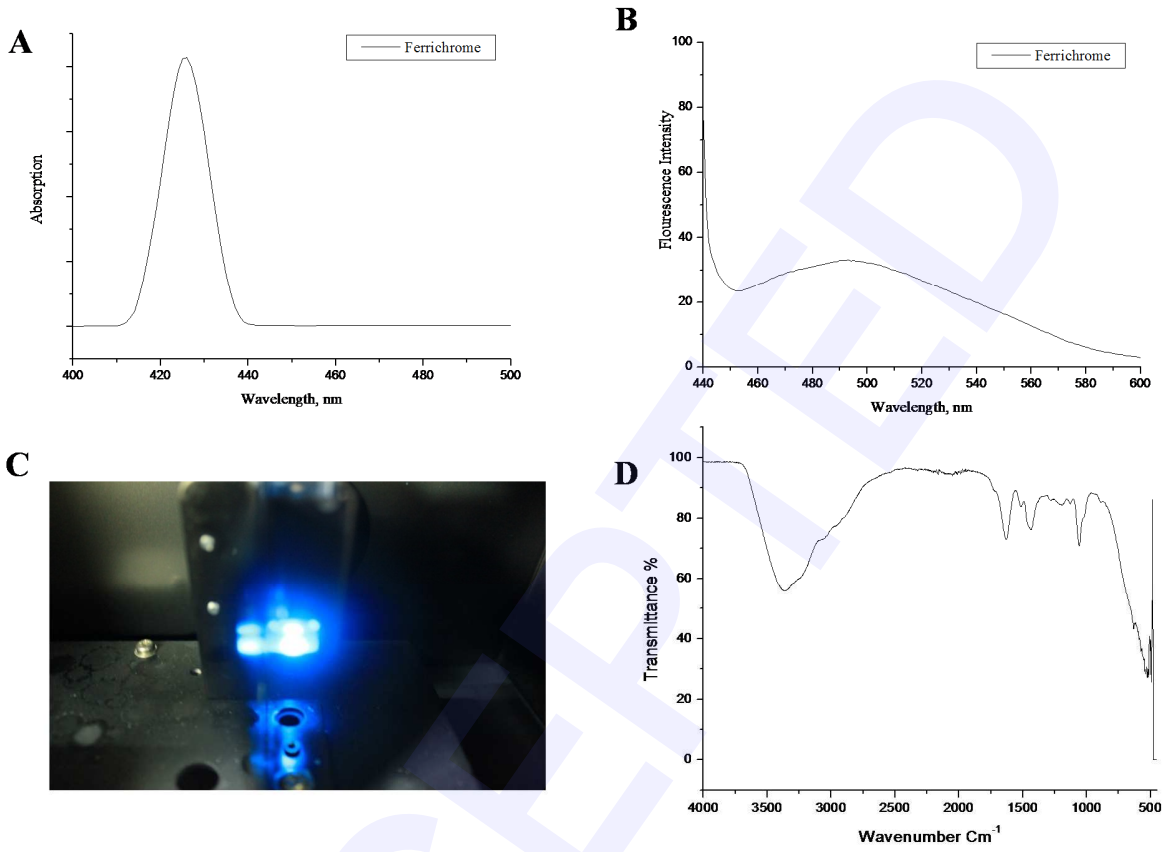

Fig. 3. Characterization of ferrichrome using spectroscopic techniques. (A) UV absorption spectroscopy. (B) Fluorescence emission at excitation 425nm. (C) Photographic emission of ferrichrome at wavelength 425nm that show blue color. (D) Shows the FTIR spectra of ferrichrome.

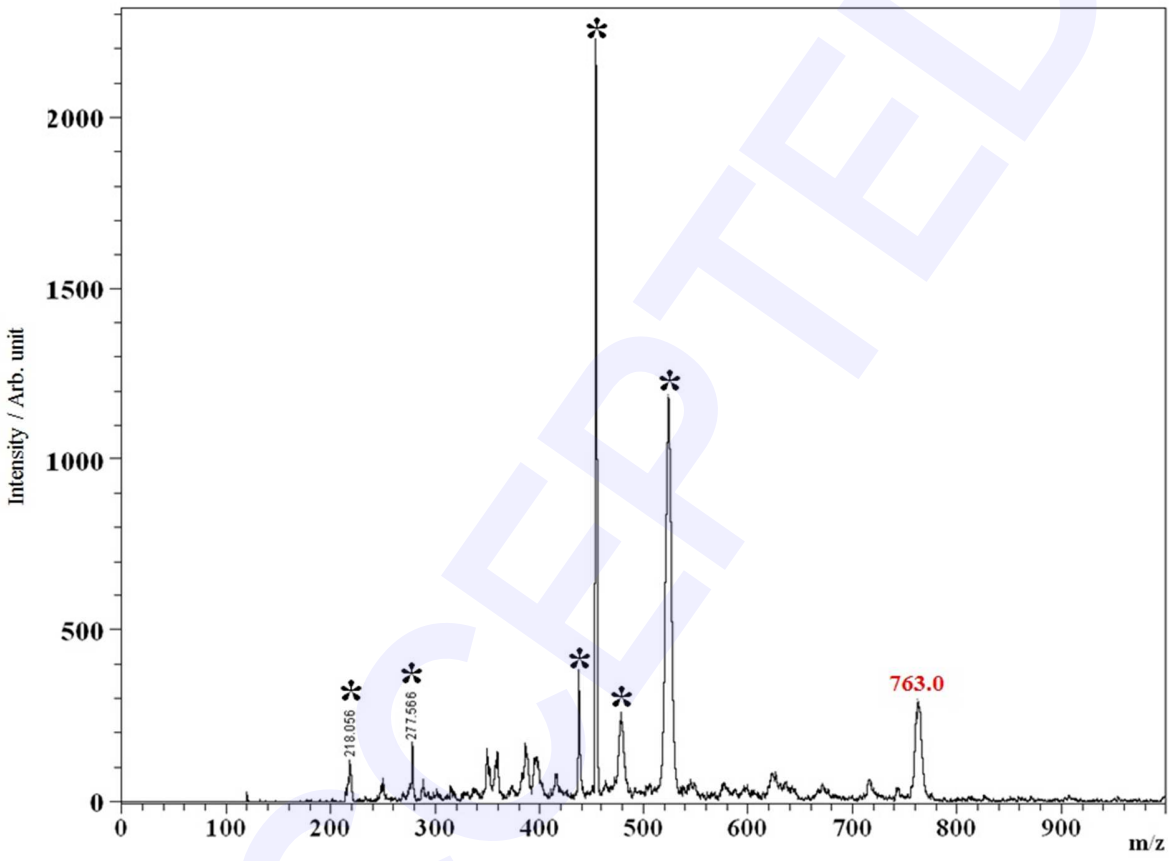

Fig. 4. MALDI-TOF-MS spectra of ferrichrome in positive mode. (*) indicates peaks corresponding to the matrix ions.

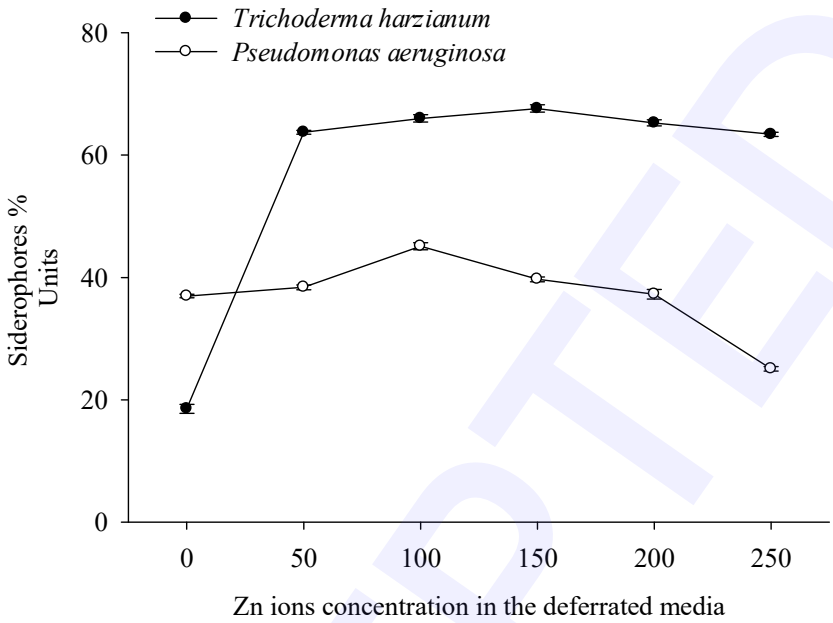

Fig. 5. Shows the optimal concentrations of Zn^{2+} ions in the deferrated media for siderophores generation by *Trichoderma harzianum* in contrast, and bacterial case.